Dual control of ROS1-mediated active DNA demethylation by the DNA DAMAGE BINDING protein 2 (DDB2)

D Córdoba-Cañero, V Cognat, R Ariza, T Roldán Arjona, Jean Molinier

▶ **To cite this version:**

D Córdoba-Cañero, V Cognat, R Ariza, T Roldán Arjona, Jean Molinier. Dual control of ROS1-mediated active DNA demethylation by the DNA DAMAGE BINDING protein 2 (DDB2). The Plant Journal, 2017, 92 (6), pp.1170-1181. ⟨hal-02289589⟩

HAL Id: hal-02289589

https://hal.science/hal-02289589v1

Submitted on 16 Sep 2019

HAL is a multi-disciplinary open access archive for the deposit and dissemination of scientific research documents, whether they are published or not. The documents may come from teaching and research institutions in France or abroad, or from public or private research centers.

L'archive ouverte pluridisciplinaire **HAL**, est destinée au dépôt et à la diffusion de documents scientifiques de niveau recherche, publiés ou non, émanant des établissements d'enseignement et de recherche français ou étrangers, des laboratoires publics ou privés.

HAL Authorization

the plant journal

SEB Society for Experimental Biology

The Plant Journal (2017) **92,** 1170–1181 doi: 10.1111/tpj.13753

Dual control of ROS1-mediated active DNA demethylation by DNA damage-binding protein 2 (DDB2)

Dolores Córdoba-Cañero[1,2,3,†], Valérie Cognat[4,†], Rafael R. Ariza[1,2,3], Teresa Roldán Arjona[1,2,3,*] and Jean Molinier[4,*]

[1]*Maimónides Biomedical Research Institute of Córdoba (IMIBIC), Av. Menéndez Pidal, 14004 Córdoba, Spain,*

[2]*University of Córdoba, Campus de Rabanales, Edif. C5, 14071 Córdoba, Spain,*

[3]*Reina Sofia University Hospital, Av. Menéndez Pidal, 14004 Córdoba, Spain, and*

[4]*Institut de Biologie Moléculaire des Plantes, 12 Rue du Général Zimmer, 67000 Strasbourg, France*

Received 13 September 2017; revised 10 October 2017; accepted 17 October 2017; published online 27 October 2017.

*For correspondence (e-mails jean.molinier@ibmp-cnrs.unistra.fr; ge2roarm@uco.es).

[†]These authors contributed equally.

SUMMARY

By controlling gene expression, DNA methylation contributes to key regulatory processes during plant development. Genomic methylation patterns are dynamic and must be properly maintained and/or re-established upon DNA replication and active removal, and therefore require sophisticated control mechanisms. Here we identify direct interplay between the DNA repair factor DNA damage-binding protein 2 (DDB2) and the ROS1-mediated active DNA demethylation pathway in *Arabidopsis thaliana*. We show that DDB2 forms a complex with ROS1 and AGO4 and that they act at the *ROS1* locus to modulate levels of DNA methylation and therefore *ROS1* expression. We found that DDB2 represses enzymatic activity of ROS1. DNA demethylation intermediates generated by ROS1 are processed by the DNA 3′-phosphatase ZDP and the apurinic/apyrimidinic endonuclease APE1L, and we also show that DDB2 interacts with both enzymes and stimulates their activities. Taken together, our results indicate that DDB2 acts as a critical regulator of ROS1-mediated active DNA demethylation.

Keywords: DDB2, AGO4, ROS1, DNA methylation, active DNA demethylation, *Arabidopsis thaliana*.

INTRODUCTION

As sessile organisms, plants are particularly exposed to the deleterious effects of environmental stress, which can affect integrity of the genome and epigenome by inducing DNA damage and chromatin alterations (Pecinka and Mittelsten Scheid, 2012). Therefore it would be of evolutionary benefit to plants to combine genome and epigenome surveillance processes, to efficiently deal with the chromosome instability that could be transmitted to the progeny. In Arabidopsis, interplays between genome and epigenome stability have been reported. Loss of function of DNA damage-binding protein 2 (DDB2), which is involved in the recognition of UV-induced DNA lesions during global genome repair (GGR; Chu and Chang, 1988; Molinier *et al.*, 2008), and of the MutS homologue 1 (MSH1), involved in mismatch repair (MMR), lead to genome-wide alterations in DNA methylation (Virdi *et al.*, 2015; Schalk *et al.*, 2016). However, the underlying mechanisms remain to be determined.

DNA methylation (5-methyl cytosine, 5-meC), a key component of the plant epigenome, contributes to the stable silencing of transposable elements (TEs) as well as to the regulation of gene expression (Law and Jacobsen, 2010). In Arabidopsis, DNA methylation is maintained by four main DNA methyltransferases: methyltransferase 1 (MET1), chromomethylase 3 (CMT3), chromomethylase 2 (CMT2) and domains rearranged methyltransferase 2 (DRM2) acting in the CG, CHG and CHH sequence contexts (where H = A, T or C), respectively (Law and Jacobsen, 2010; Zemach *et al.*, 2013). Additionally, cytosines can be methylated *de novo* through RNA-directed DNA methylation (RdDM) involving different classes of small RNA (Cuerda-Gil and Slotkin, 2016). RdDM transcriptionally represses TEs and is involved in heterochromatin formation (Matzke and Mosher, 2014).

DNA methylation is a reversible process (Zhu, 2009). Upon DNA replication and in the absence of *de novo* and/or maintenance pathways DNA methylation can be passively lost (Zhu, 2009). Additionally, specific enzymes can also reduce DNA methylation in a cognate base excision repair (BER) mechanism (Zhu, 2009). This pathway, called

© 2017 The Authors
The Plant Journal published by John Wiley & Sons Ltd and Society for Experimental Biology.
This is an open access article under the terms of the Creative Commons Attribution License, which permits use, distribution and reproduction in any medium, provided the original work is properly cited.

active DNA demethylation, counteracts RdDM and mainly prevents the spread of DNA methylation (Penterman *et al.*, 2007; Matzke and Mosher, 2014). In Arabidopsis, active DNA demethylation can be achieved by four specific 5-meC DNA glycosylases, repressor of silencing 1 (ROS1), demeter (DME), demeter like-2 (DML2) and demeter like-3 (DML3; Zhu, 2009). These enzymes remove 5-meC and cleave the phosphodiester backbone by either β- or β, δ-elimination, generating single-nucleotide gaps with either 3′-PUA (3′-phosphor-α, β-unsaturated aldehyde) or 3′-P (3′-phosphate) ends, respectively (Morales-Ruiz *et al.*, 2006). These non-canonical 3′ termini are converted to 3′-OH ends by the apurinic/apyrimidinic (AP) endonuclease APE1L (Lee *et al.*, 2014; Li *et al.*, 2015a) and the 3′ DNA phosphatase ZDP (Martínez-Macías *et al.*, 2012), respectively, allowing the subsequent DNA polymerization and ligation steps needed to complete the active demethylation process.

In order to prevent abnormal alterations of DNA methylation patterns, expression of DNA demethylases is under the complex control of different pathways (Penterman *et al.*, 2007). Expression of DML3, for example, is regulated post-transcriptionally by the microRNA miR402 (Kim *et al.*, 2010). Conversely, expression of ROS1 is regulated transcriptionally by a complex balance between DNA methylation and active DNA demethylation involving a particular sequence in the ROS1 promoter region called the DNA methylation monitoring sequence (MEMS), which serves as a methyl-rheostat (Lei *et al.*, 2015; Williams *et al.*, 2015). DNA methylation of MEMS activates expression of ROS1 whilst active DNA demethylation of MEMS represses it (Lei *et al.*, 2015; Williams *et al.*, 2015). Active DNA demethylation can also be controlled via regulation of DNA glycosylase/AP lyase activity. ROS1 contains an iron–sulfur cluster-binding motif that is essential for its enzymatic activity (Duan *et al.*, 2015; Wang *et al.*, 2016). Moreover, the iron–sulfur cluster assembly protein MET18 interacts with ROS1 and stimulates its activity (Duan *et al.*, 2015; Wang *et al.*, 2016).

Given that active DNA demethylation is related to the BER pathway, it is likely that BER factors play an important role. Indeed, the BER protein XRCC1 was shown to interact with ROS1 and ZDP and stimulate their enzymatic activities (Martínez-Macías *et al.*, 2013), thus strengthening the idea that specific DNA repair factors may act as key regulatory elements of DNA demethylation.

We have recently reported that DDB2 loss of function induces alterations in DNA methylation arising partially from *ROS1* upregulation (Schalk *et al.*, 2016). Interestingly DDB2 also controls *de novo* DNA methylation by interacting with the RdDM factor AGO4 (Schalk *et al.*, 2016). Given that *ROS1* expression is under the control of RdDM and active DNA demethylation we hypothesized that DDB2 may play a role in such antagonistic regulatory processes.

Here, we decipher an interplay between DDB2, AGO4 and the ROS1-mediated active DNA demethylation pathway at the *ROS1* locus. We unveil that DDB2 together with ROS1 and AGO4 form a complex *in planta*. This, at least, tripartite complex acts predominantly at MEMS of the *ROS1* locus, modulating its DNA methylation levels. We found that DDB2 interacts directly with ROS1 and inhibits its enzymatic activity. Moreover, we show that DDB2 also directly interacts with two downstream DNA demethylation factors, ZDP and APE1L, and stimulates their activities. Collectively, these results suggest that the GGR factor DDB2 has an important function during ROS1-mediated active DNA demethylation via the dual control of *ROS1* expression and activity.

RESULTS

DDB2 represses *ROS1* expression

Expression of *ROS1* was shown to be promoted by DNA methylation and antagonized by active DNA demethylation pathways (Lei *et al.*, 2015; Williams *et al.*, 2015). Interestingly upregulation of *ROS1* was observed in plants defective for the expression of the GGR factor DDB2 (Schalk *et al.*, 2016), suggesting that this DNA repair protein acts, directly or indirectly, as a repressor of *ROS1* expression. In addition, DDB2 interconnects with the RdDM pathway via its interaction with AGO4 and therefore represents a material of choice for deciphering the underlying mechanisms of control of *ROS1* expression. Examination of the DNA methylation profile obtained by whole-genome bisulfite sequencing (WGBS; Schalk *et al.*, 2016) of the *ROS1* locus revealed that, in *ddb2* mutant plants, two regions exhibit alteration of DNA methylation profiles compared with wild-type (WT) plants (Figure 1a). One hypomethylated region (proximal, P) overlaps with the MEMS (Lei *et al.*, 2015; Williams *et al.*, 2015; Figure 1a). Another region (distal, D) is located towards the 3′ end of the coding region, between exons 15 and 17, and shows an enhanced DNA methylation level in *ddb2* mutant plants (Figure 1a). Similar alterations of DNA methylation profiles are also identified in another *ddb2* allelic mutant (Nossen ecotype), confirming the above-described trends (Figure S1a). These observations allow us to postulate that DDB2 controls DNA methylation levels at these two particular regions, and therefore *ROS1* expression. In order to characterize the underlying molecular mechanisms, we analyzed small RNA deep sequencing data (Schalk *et al.*, 2016) and identified that 24-nucleotide (nt) siRNAs overlap with the P and D regions (Figure 1a and Figure S1a in the Supporting Information). We found that abundance of 24-nt siRNA is reduced in the P region but a significant increase is detected in the D region in the *ddb2* mutant plants compared with WT plants (Figure 1a). These data are in agreement with the well-characterized direct correlation

© 2017 The Authors
The Plant Journal published by John Wiley & Sons Ltd and Society for Experimental Biology.,

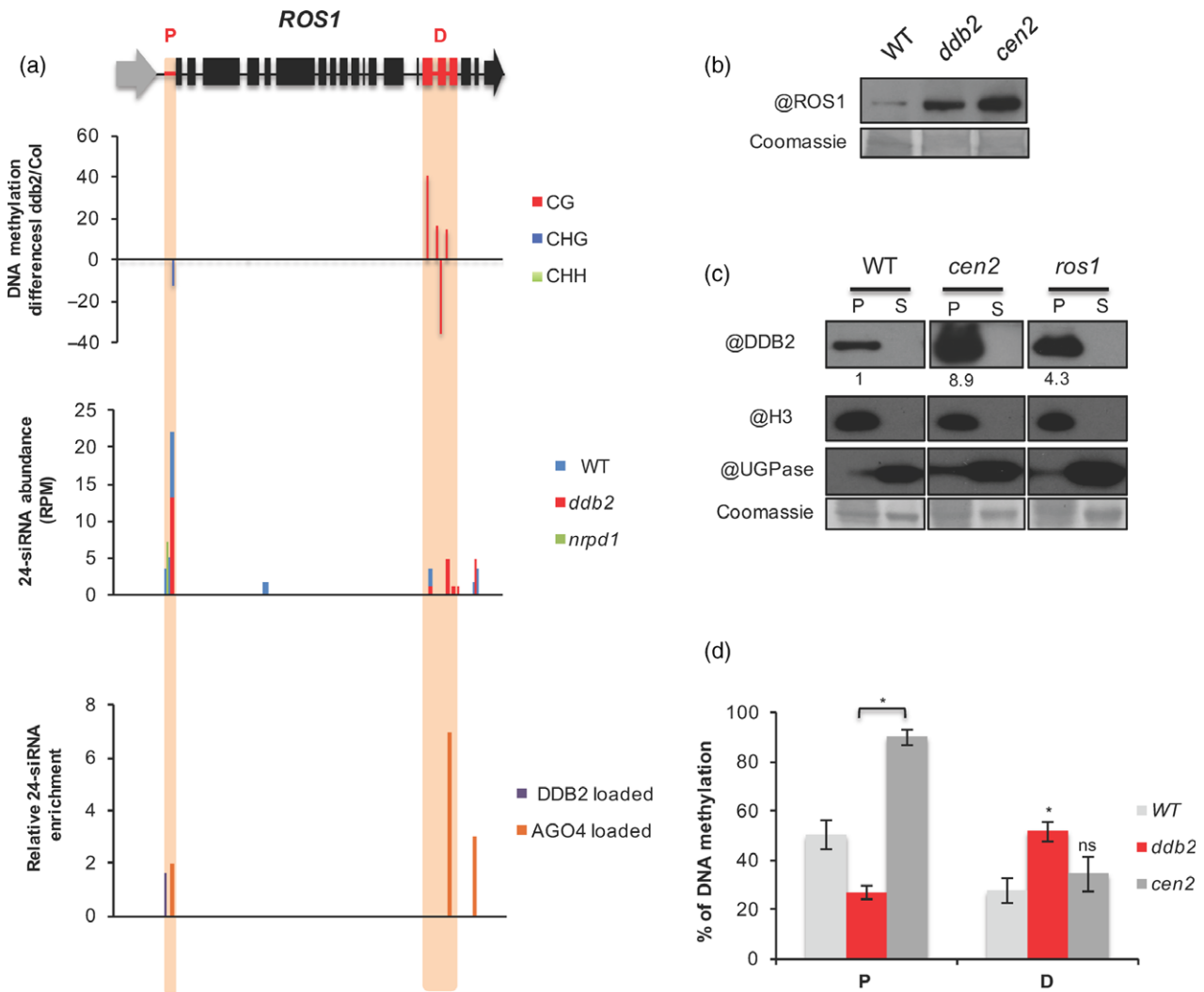

Figure 1. DNA methylation and small RNA profiles at the *ROS1* locus.
(a) Top panel: schematic representation of the *ROS1* locus. Exons and introns are shown as boxes and lines, respectively. The REP5 transposon is shown in grey. Regions exhibiting significant changes in DNA methylation levels (regions P and D) are highlighted in red. Bottom panels: schematic representation of the DNA methylation level obtained by whole-genome bisulfite sequencing for the *ROS1* locus in *ddb2-3* plants. The histograms represent hyper/hypomethylation (at least 10% difference) in *ddb2-3* plants compared with wild-type (WT; Col) plants for a 100-bp window for the P and D regions, the abundance of 24-nt siRNAs at the *ROS1* locus in WT (Col), *ddb2-3* and *nrpd1* plants and relative 24-nt siRNA enrichments in DDB2 and AGO4 RIP.
(b) Immunodetection of the ROS1 protein in WT (Col), *ddb2* and *cen2* plants. Coomassie blue staining of the blot is shown.
(c) Immunoblot analysis of DDB2 protein content associated with the insoluble chromatin fraction (P, pellet) and the soluble fraction (S, supernatant) from WT, *cen2* and *ros1* plants. Anti-histone H3 and anti-UGPase antibodies were used as controls for insoluble (P) and soluble fractions (S), respectively. Signal intensity relative to H3 or Coomassie is indicated below each lane. Coomassie blue staining of the blot is shown.
(d) Percentage of DNA methylation in WT (Col), *ddb2* and *cen2* plants for P and D regions of the *ROS1* locus. Data are presented as percentage of methylation (±SD) determined by McrBC-qPCR and are representative of three biological replicates. *t*-test $*P < 0.01$; ns, non-significant compared with WT (Col).

between 24-nt siRNA abundance and DNA methylation level (Matzke and Mosher, 2014). In addition, using DDB2-FLAG immunoprecipitation followed by small RNA-seq (RIP; Schalk *et al.*, 2017) and publicly available AGO4 RIP data (Mi *et al.*, 2008), we identified that the 24-nt siRNAs matching with the P region are loaded into a DDB2- and/or an AGO4-containing complex whereas those matching with the D region are exclusively loaded into AGO4 (Figure 1a). These results are consistent with the differential 24-nt siRNA abundance measured in WT and *ddb2* plants at the P and D regions (Figure 1a). These data support the idea that DNA methylation levels of these two regions are under the control of DDB2 and/or AGO4 siRNAs and may play an important role in the regulation of *ROS1* expression.

To further examine the contributions of RdDM, active DNA demethylation and DDB2 to the control of *ROS1* expression we tested the DNA methylation levels of P and D regions in double *ddb2-nrpd1* and *ddb2-ros1* plants. McrBC-quantitative PCR (qPCR) analyses showed that

© 2017 The Authors

ddb2-induced DNA hypomethylation in the P region and DNA hypermethylation in the D region reverted to WT levels in both *ddb2-nrpd1* and *ddb2-ros1* double-mutant plants (Figure S1b, c). The strong reduction in *ROS1* expression levels in *ddb2-nrpd1* plants (Figure S1b) despite the WT level of DNA methylation indicates that DNA methylation may not be the only factor influencing the steady-state level of *ROS1* mRNA. In addition, our results highlight that DDB2- and ROS1-mediated active DNA demethylation act antagonistically at the P region whereas both factors may negatively control *de novo* DNA methylation at the D region.

Depletion of the cognate GGR factor, CEN2, also leads to enhanced *ROS1* expression (Schalk and Molinier, 2016; Figure 1b). Interestingly CEN2 influences DDB2 homeostasis (Matsumoto *et al.*, 2015). Indeed, a higher chromatin DDB2 content could be detected in *cen2* plants compared with WT plants (Figure 1c). Therefore, *cen2* mutant plants represent a material of choice to better assess the role of DDB2 in the control of *ROS1* expression. Thus we compared the DNA methylation levels of the P and D regions in WT, *ddb2* and *cen2* plants using McrBC-qPCR. Unlike *ddb2* plants, *cen2* plants, exhibit a higher DNA methylation level exclusively at the P region compared with WT plants and not at the D region (Figure 1d), consistent with the direct correlation between DNA methylation of the MEMS, overlapping the P region, and *ROS1* expression (Lei *et al.*, 2015). In addition, this strongly suggests that a prospective direct correlation may exist between DDB2 chromatin content and DNA methylation levels.

Taken together, these results strengthen the idea that control of *ROS1* expression is regulated by a complex DNA methylation-based process in which GGR factors, and probably DDB2, play a crucial role. These results also suggest that the D region may serve as back-up rheostat to control *ROS1* expression.

DDB2, ROS1 and AGO4 act directly at the *ROS1* locus

The above results indicate that GGR factors influence DNA methylation levels predominantly at the P region (MEMS), and highlight that the D region, in the absence of DDB2, may play a secondary role in the control of *ROS1* expression. To further explore the relationship between DNA methylation levels at these particular regions and local enrichment of DDB2 and of key effectors of the DNA methylation/demethylation processes, we performed chromatin immunoprecipitation (ChIP) experiments in a set of Arabidopsis mutant plants.

Using DDB2-FLAG-expressing plants (Schalk *et al.*, 2016), ChIP-qPCR analyses revealed a significant enrichment of DDB2 in the P region whereas no difference was detectable in the D region compared with WT control plants (Figure 2a). Interestingly, in *rdr2* DDB2-FLAG-expressing plants, in which AGO4 and ROS1 are not expressed (Penterman *et al.*, 2007), DDB2 enrichment in the P region was enhanced compared with DDB2-FLAG plants (Figure 2a). These data are correlated with the higher DDB2 chromatin contents found in *ago4* plants (Schalk *et al.*, 2016). Conversely, no significant difference in DDB2-FLAG enrichment was measured for the D region (Figure 2a) suggesting an indirect effect on the DNA methylation level.

Similarly to *cen2* and *ago4* plants, DDB2 chromatin content is higher in *ros1* plants than in WT plants (Figure 1c), suggesting that ROS1 may also influence DDB2 chromatin enrichment. Thus we investigated DDB2 content at the *ROS1* locus in *cen2* and *ros1* DDB2-FLAG-expressing plants. For the P and D regions DDB2 enrichment was around the background level in both *cen2* and *ros1* plants (Figure 2a). This indicates that DDB2 binding at the P region requires CEN2 and ROS1. Moreover, these data highlight that ROS1 and CEN2 similarly influence local (*ROS1* locus) and global DDB2 chromatin content.

Given that interconnection exists between RdDM and DDB2 (Schalk *et al.*, 2016) and that *ROS1* expression is promoted by DNA methylation we performed ChIP experiments using anti-AGO4 antibody in WT and *ddb2* plants. In WT plants AGO4 enrichment was exclusively observed in the D region, whereas in *ddb2* plants it was enhanced for both regions (Figure 2b). This observation is compatible with a possible direct correlation between the specific AGO4 content at the D region and the enhanced 24-nt siRNA abundance identified in *ddb2* plants (Figure 1a). Moreover, these findings strengthen the idea that DDB2 may act as a chaperone for AGO4, possibly controlling its availability on chromatin for DNA methylation effectors.

ROS1 expression was shown to be antagonized by itself at MEMS (Lei *et al.*, 2015). Therefore, we tested the chromatin association of ROS1 with the P and D regions in *ros1*, *ddb2* or *cen2* plants expressing C-terminal FLAG-tagged ROS1 protein. The ChIP-qPCR analyses revealed a significant enrichment of ROS1-FLAG in the P and D regions (Figure 2c) confirming the results of Lei *et al.* (2015). Interestingly, in *ddb2* mutant plants, ROS1-FLAG enrichment was enhanced in the P region whereas no significant change was detectable for the D region (Figure 2c). These data are correlated with the putative direct relationship between local enhancement of ROS1 content in the P region (Figure 2c) and its reduced DNA methylation level measured in *ddb2* plants (Figure 1d). Conversely, *cen2* plants exhibit reduced ROS1 enrichment in the P and D regions compared with *ros1* ROS1-FLAG and *ddb2* ROS1-FLAG plants (Figure 2c) that directly correlates with the DNA methylation levels measured in *cen2* plants (Figure 1d).

Taken together, these ChIP experiments allow DDB2 to be added as a new local player in the control of *ROS1*

© 2017 The Authors
The Plant Journal published by John Wiley & Sons Ltd and Society for Experimental Biology.,

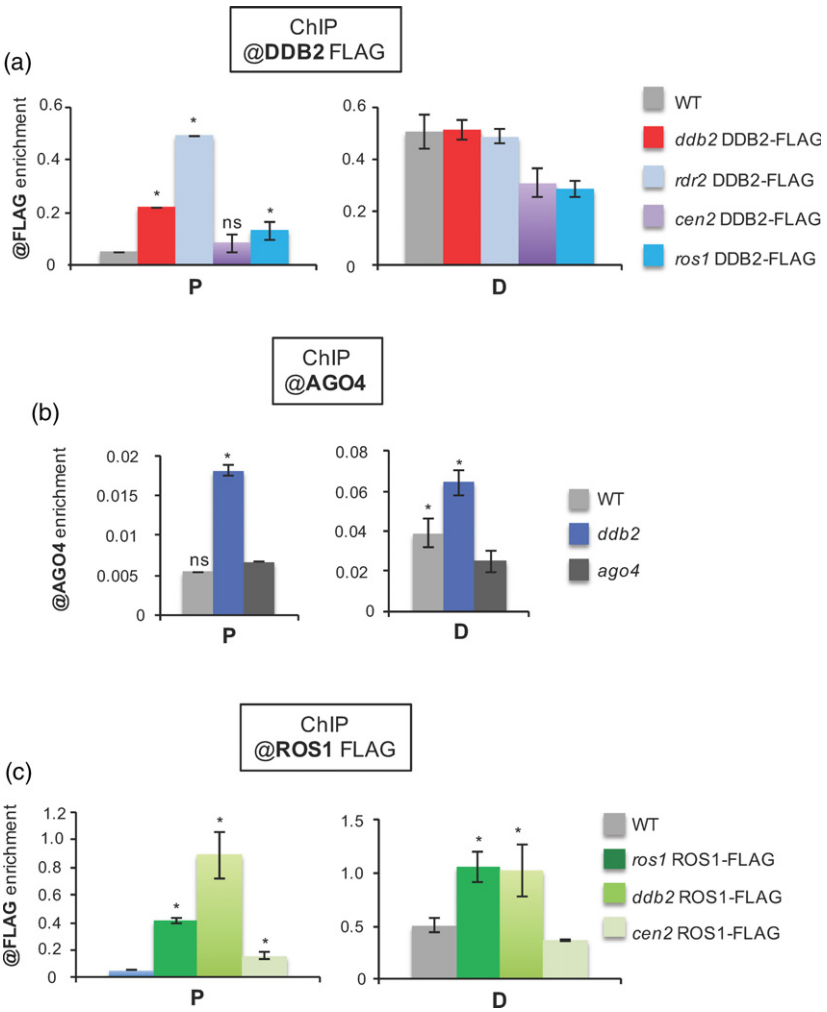

Figure 2. Enrichment of DDB2, AGO4 and ROS1 at the *ROS1* locus.
(a) Chromatin immunoprecipitation (ChIP)-quantitative (q)PCR analysis of DDB2 enrichment at the P and D regions of the *ROS1* locus in *ddb2 DDB2-FLAG-*, *rdr2 DDB2-FLAG-*, *cen2 DDB2-FLAG-* and *ros1 DDB2-FLAG*-expressing plants.
(b) ChIP-qPCR analysis of AGO4 enrichment in wild-type (WT; Col) and *ddb2* plants. *t*-test $*P < 0.01$; ns, non-significant compared with *ago4* plants.
(c) ChIP-qPCR analysis of ROS1 enrichment in *ros1 ROS1-FLAG-*, *ddb2 ROS1-FLAG-* and *cen2 DDB2-FLAG*-expressing plants. WT plants were used as negative controls for DDB2-FLAG and ROS1-FLAG ChiP. *ago4* plants were used as a negative control for AGO4 ChIP. *t*-test $*P < 0.01$; ns, non-significant compared with WT (Col). Data are presented as enrichment of FLAG/AGO4 signal (±SD) and are representative of three biological replicates.

expression together with ROS1 and AGO4. Interestingly, our data shed light on a complex co-regulation of DDB2, ROS1 and AGO4 contents predominantly at the P region and more moderately at the D region. We propose that there is subtle regulation of the availability and stability of DDB2, ROS1 and AGO4 which modulates *ROS1* expression, probably through fine tuning of DNA methylation profiles.

ROS1 interacts with DDB2 and AGO4

Given that ROS1 and DDB2 bind DNA directly, and that both proteins are enriched at the P region of *ROS1*, we wondered whether DDB2 could physically interact with ROS1. Using *in vitro* pull-down experiments, we demonstrated that ROS1 interacts directly with DDB2 (Figure 3a). In addition, the ROS1-FLAG protein co-immunoprecipitated with endogenous DDB2 protein (Figure 3b), confirming the aforementioned *in vitro* data. ROS1-dependent active DNA demethylation antagonizes RdDM (Zhu, 2009; Tang *et al.*, 2016). Since DDB2 interacts directly with ROS1 and also assembles with AGO4 in a high-molecular-weight complex (Schalk *et al.*, 2016), it is possible that these three proteins are part of the same protein complex. Indeed, endogenous DDB2 and AGO4 co-immunoprecipitated with ROS1-FLAG (Figure 3c). Collectively, these data provide compelling evidence that ROS1, DDB2 and AGO4 form a complex that may trigger either silencing or anti-silencing at particular loci.

DDB2 inhibits ROS1 5-meC DNA glycosylase activity

Since DDB2 and ROS1 interact both *in vitro* and *in vivo*, we asked whether DDB2 exerts any effect on the enzymatic activity of ROS1. ROS1 was incubated, in either the absence or the presence of DDB2, with a 51-mer duplex oligo substrate that contained a 5-meC:G at position 29 (Figure 4a). ROS1 is a bifunctional DNA glycosylase/AP lyase that catalyzes both the release of 5-meC and the subsequent cleavage of DNA at the resulting abasic site by β,δ-elimination (Morales-Ruiz *et al.*, 2006). In this assay, the 5-meC DNA glycosylase/lyase activity is detected by the

© 2017 The Authors

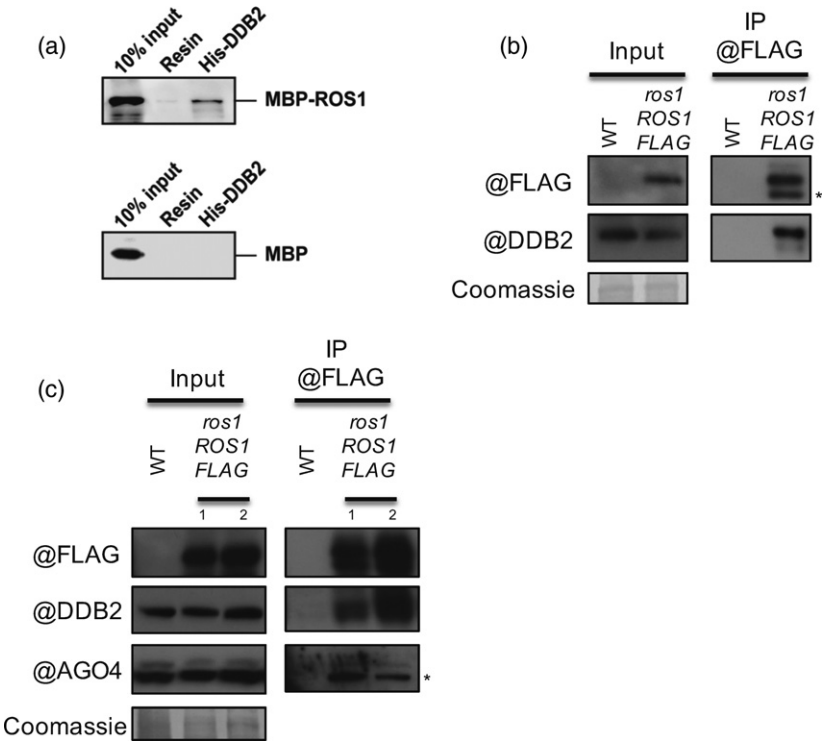

Figure 3. ROS1 interacts with DDB2 and AGO4.
(a) *In vitro* pull down of ROS1 with DDB2 protein. Purified DDB2 fused to a His tag was fixed to a Ni-Sepharose column and incubated with either MBP-ROS1 or MBP. After washes, the proteins associated with the resin were separated by SDS-PAGE, transferred to a membrane and immunoblotted with antibodies against MBP.
(b) *In vivo* pull-down of ROS1 with DDB2 protein. WT (Col) and *ros1 ROS1-FLAG* plants were used for immunoprecipitation assays using anti-FLAG antibody. Coomassie blue staining of the blot is shown. *Cross-reacting signal.
(c) *In vivo* pull-down of ROS1 with DDB2 and AGO4 proteins. WT (Col) and *ros1 ROS1-FLAG* expressing plants were used for immunoprecipitation assays using anti-FLAG antibody. Coomassie blue staining of the blot is shown. *Cross-reacting signal.

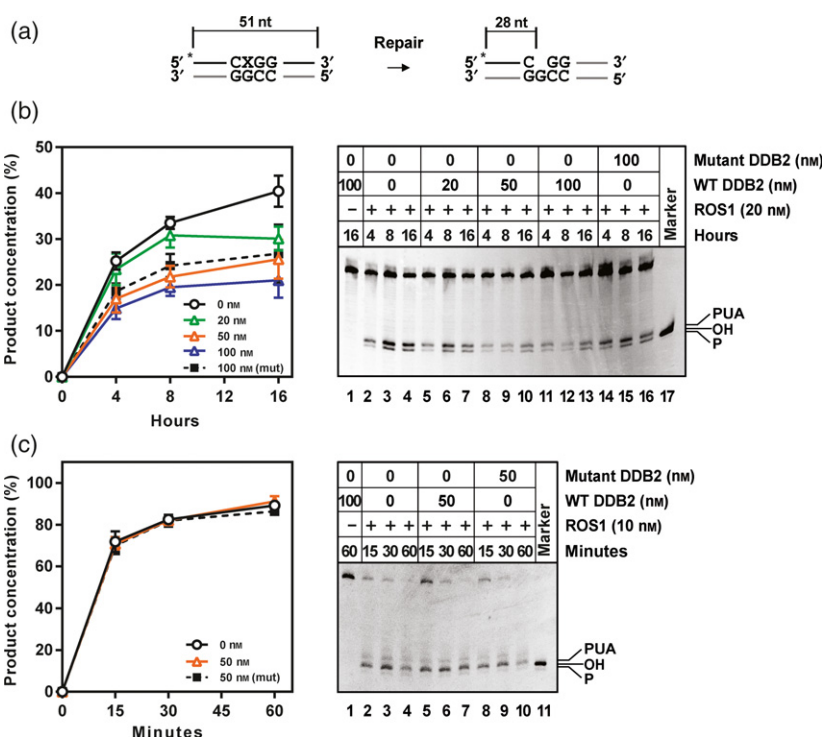

Figure 4. DDB2 inhibits ROS1 5-meC DNA glycosylase activity.
(a) Schematic diagram of molecules used as DNA substrates. Double-stranded oligonucleotides containing either a single 5-meC or an AP site (indicated as X) on the upper strand. The fluor-labeled 5′-end of the upper strand is indicated by an asterisk. The size of the 5′-end labeled fragment generated after DNA glycosylase/lyase activity is indicated.
(b) DDB2 inhibits the DNA glycosylase activity of ROS1. Purified ROS1 was incubated with a double-stranded oligonucleotide substrate containing a single 5-meC at the 5′-end-labeled upper strand, in the absence or presence of purified wild-type (WT) or mutant versions of DDB2. Graph data on the left are mean ± SE from three independent experiments. A representative gel is shown on the right.
(c) DDB2 has no effect on the AP lyase activity of ROS1. Purified ROS1 was incubated with a double-stranded oligonucleotide substrate containing an AP site at the 5′-end-labeled upper strand, in the absence or the presence of purified WT and mutant versions of DDB2. Graph data on the left are mean ± SE from three independent experiments. A representative gel is shown on the right.

appearance of 28-nt incision products with either 3′-PUA or 3′-P ends. We observed that increasing amounts of DDB2 strongly inhibit the processing of 5-meC by ROS1 (Figure 4b).

Although the base excision and strand incision steps catalyzed by ROS1 are highly coordinated (Ponferrada-Marín *et al.*, 2009), they are the result of separate DNA glycosylase and AP lyase activities that can be uncoupled by

© 2017 The Authors

mutation of specific residues (Parrilla-Doblas *et al.*, 2013). We therefore asked whether DDB2 inhibits either the DNA glycosylase activity or the AP lyase activity of ROS1. To specifically detect ROS1 AP lyase activity, we performed enzymatic reactions with an analogous DNA substrate containing an abasic site instead of the target 5-meC at position 29 (Figure 4c). The results show that DDB2 does not exert any detectable effect on ROS1 AP lyase activity. Taken together, these results indicate that DDB2 specifically inhibits the 5-meC excision step catalyzed by ROS1.

Since both DDB2 and ROS1 have DNA-binding capacity, we next asked whether the inhibitory effect of DDB2 on the 5-meC excision activity of ROS1 could be a consequence of competition for the DNA substrate. To test this hypothesis, the 5-meC-containing DNA was either pre-incubated or not with DDB2 before adding ROS1 to the reaction mixture (Figure S2). We found that pre-incubating the DNA substrate with DDB2 does not increase ROS1 inhibition, which argues against a simple competition effect. This result is in agreement with the fact that a K314E-mutated form of DDB2, which is impaired in DNA-binding (Schalk *et al.*, 2016), retains most of the inhibitory capacity exerted by WT DDB2 on ROS1 (Figure 4b, c). Taken together, these results suggest that DDB2 directly inhibits excision of 5-meC catalyzed by ROS1.

DDB2 stimulates post-incision events in the DNA demethylation pathway

The plant DNA demethylation pathway initiated by ROS1 is a multistep BER process in which additional proteins are required to catalyze downstream repair stages that culminate in the replacement of 5-meC with unmethylated C. As indicated above, the product generated by ROS1 is a single-nucleotide gap with either 3′-P or 3′-PUA ends. These non-canonical 3′ termini must be converted to 3′-OH ends before DNA polymerase and ligase activities can complete DNA demethylation. We have previously reported that the DNA 3′-phosphatase ZDP removes the blocking 3′-P, allowing subsequent DNA polymerization and ligation steps needed to complete demethylation. Furthermore, ZDP and ROS1 interact *in vitro* and co-localize *in vivo* (Martínez-Macías *et al.*, 2012). We therefore asked whether DDB2 exerts any effect on the DNA-3′ phosphatase activity of ZDP. Purified ZDP was incubated with a 5′-end-labeled single-nucleotide gapped substrate (Table S1), either in the absence or presence of DDB2, and measured the conversion from 3′-P to 3′-OH (Figure 5a). Interestingly, and in stark contrast to the effect on ROS1, we found that DDB2 stimulates ZDP activity. In the absence of ZDP, the DDB2 protein showed no detectable activity on the gapped

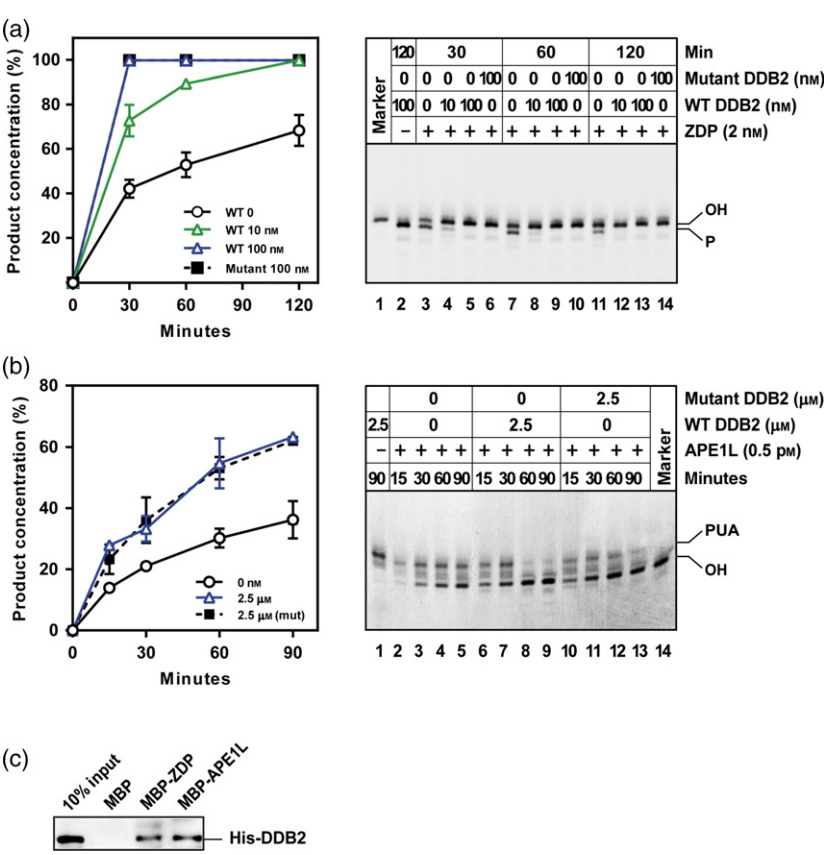

Figure 5. DDB2 stimulates post-incision events during the DNA demethylation pathway.
(a) DDB2 stimulates the DNA 3′-phosphatase activity of ZDP. Purified ZDP was incubated with a double-stranded oligonucleotide substrate containing a single-nucleotide gap flanked by 3′-phosphate and 5′-phosphate ends at the 5′-end-labeled upper strand, in the absence or presence of purified WT or mutant versions of DDB2. Graph data on the left are mean ± SE from three independent experiments. A representative gel is shown on the right.
(b) DDB2 stimulates the 3′-phosphodiesterase activity of APE1L. Purified APE1L was incubated with a double-stranded oligonucleotide substrate containing a single-nucleotide gap flanked by 3′-PUA and 5′-phosphate ends at the 5′-end-labeled upper strand, in the absence or presence of purified WT or mutant versions of DDB2. Graph data on the left are mean ± SE from three independent experiments. A representative gel is shown on the right.
(c) DDB2 interacts with ZDP and APE1L. Purified ZDP and APE1L fused to MBP, or MBP alone, were fixed to an amylose column. The proteins bound to the column were incubated in the presence of His-DDB2. After washes, the proteins associated with the resin were separated by SDS-PAGE, transferred to a membrane and immunoblotted with antibodies against the His-tag.

© 2017 The Authors
The Plant Journal published by John Wiley & Sons Ltd and Society for Experimental Biology.,

substrate (Figure 5a, lane 2), suggesting that the enhanced activity indicates stimulation of ZDP.

The other types of non-canonical 3′-termini generated by ROS1 are 3′-PUA ends. We have previously shown that APE1L, one of three Arabidopsis AP endonucleases, has a potent 3′-phosphodiesterase activity that processes the 3′-PUA blocking groups to generate 3′-OH. Furthermore, APE1L and ROS1 interact *in vitro* and *in vivo* (Li *et al.*, 2015a). To test the effect of DDB2 on the 3′-phosphodiesterase activity of APE1L we incubated both proteins, either singly or in combination, with a 5′-end-labeled DNA gapped substrate containing a 3′-end and measured its conversion to 3′-OH (Figure 5b). We found that DDB2 enhances APE1L activity, although at higher concentrations than those required to stimulate ZDP. In the absence of APE1L, the DDB2 protein exhibited no detectable activity on 3′-PUA ends (Figure 5b, lane 1), suggesting that the enhanced activity indicates stimulation of APE1L. APE1L is also endowed with a weak AP-endonuclease activity that was not affected by DDB2 (Figure S3a).

The K314E mutated form of DDB2 retains the stimulatory capacity exerted by WT DDB2 either on ZDP or APE1 (Figure 5), which suggests that stimulation is independent of DNA-binding by DDB2. We performed *in vitro* pull-down assays to prove a direct interaction between DDB2 and either ZDP or APE1L. As shown in Figure 5(c), MBP-ZDP and MBP-APE1L, but not MBP alone, bound to His-DDB2. Taken together, these results suggest that DDB2 interacts directly with ZDP and APE1L and stimulates their 3′-phosphatase and 3′-phosphodiesterase activity, respectively.

We also examined the possible effect of DDB2 on additional stages of the DNA demethylation pathway. The DNA polymerase(s) responsible for gap filling have not yet been identified, but it has been reported that the final ligation step is catalyzed by LIG1 (Córdoba-Cañero *et al.*, 2011; Li *et al.*, 2015b). However, we could not detect any effect of DDB2 on LIG1 DNA ligase activity (Figure S3b). Collectively, these results suggest that DDB2 stimulates post-incision events during the DNA demethylation pathway, which may help to avoid accumulation of repair intermediates with blocked 3′-ends.

DISCUSSION

In this study we demonstrate that DDB2 contributes to the control of *ROS1* expression through fine-tuning of the DNA methylation level of the *ROS1* locus. We reveal that ROS1, DDB2 and AGO4 form a complex *in vivo*, allowing DDB2 to mediate a sophisticated control of RdDM and of active DNA demethylation pathways predominantly at MEMS (Figure 6a). Moreover, we unveil that DDB2 directly interacts with three components of the active demethylation pathway, ROS1, ZDP and APE1L, inhibiting ROS1 glycosylase activity and stimulating ZDP and APE1L activities (Figure 6b). Taken together, our results strengthen the notion that a direct interplay exists between DNA repair and DNA methylation dynamics.

DDB2 controls active DNA demethylation

Our analyses show that DDB2 acts at several stages during active DNA demethylation. We demonstrated that DDB2 interacts *in vitro* and *in vivo* with ROS1 and inhibits its 5-meC DNA glycosylase activity. This differs from the stimulatory effect reported for other ROS1 interactors (Martínez-Macías *et al.*, 2013; Duan *et al.*, 2015; Wang *et al.*, 2016). Interestingly, we found that the inhibitory effect of DDB2 is not a consequence of direct competition between ROS1 and DDB2 for the DNA substrate. It would thus be interesting to map the DDB2–ROS1 interaction domains in order to better decipher how the enzymatic activity of ROS1 is inhibited. Upon removal of 5-meC, gaps flanked by 3′-P or 3′-PUA blocking ends are generated and must be processed to allow efficient gap filling and DNA ligation (Martínez-Macías *et al.*, 2012; Li *et al.*, 2015a). We found that DDB2 interacts with the Arabidopsis DNA phosphatase ZDP and AP endonuclease APE1L, stimulating their activities. The intrinsic capacity of DDB2 to bind changes in DNA structure (Wittschieben *et al.*, 2005) may explain why DDB2 acts at this step of the active DNA demethylation process. This result allows us to speculate that, by sensing DNA demethylation intermediates, DDB2 could be a general factor in active DNA demethylation including DME-, DML2- and DML3-mediated processes. Another DNA repair factor, XRCC1, which acts as a scaffolding protein during BER, interacts with ZDP and stimulates its enzymatic activity (Martínez-Macías *et al.*, 2013). Together these data stress the point that, as a DNA repair process, many factors related to short/long patch BER or NER may contribute to active DNA demethylation.

DDB2-mediated control of *ROS1* expression

Expression of *ROS1* is under the complex influence of DNA methylation and active DNA demethylation pathways (Penterman *et al.*, 2007; Lei *et al.*, 2015; Williams *et al.*, 2015). The DNA methylation level of the MEMS is positively correlated with *ROS1* expression (Lei *et al.*, 2015; Williams *et al.*, 2015). In this system, ROS1 counteracts RdDM to remove methylation at its own promoter. Therefore, factors that simultaneously influence DNA methylation and active DNA demethylation may represent putative key sophisticated regulators of *ROS1* expression. Indeed, the GGR factor DDB2 also carries such dual features. DDB2 was shown to influence *de novo* DNA methylation by controlling the local abundance of 24-nt siRNAs via interaction with AGO4 (Schalk *et al.*, 2016) as well as to repress ROS1 activity (this study).

Given that DNA methylation at MEMS is targeted by ROS1-dependent active demethylation, the slight but significant loss of DNA methylation detected at the MEMS in

© 2017 The Authors
The Plant Journal published by John Wiley & Sons Ltd and Society for Experimental Biology.,

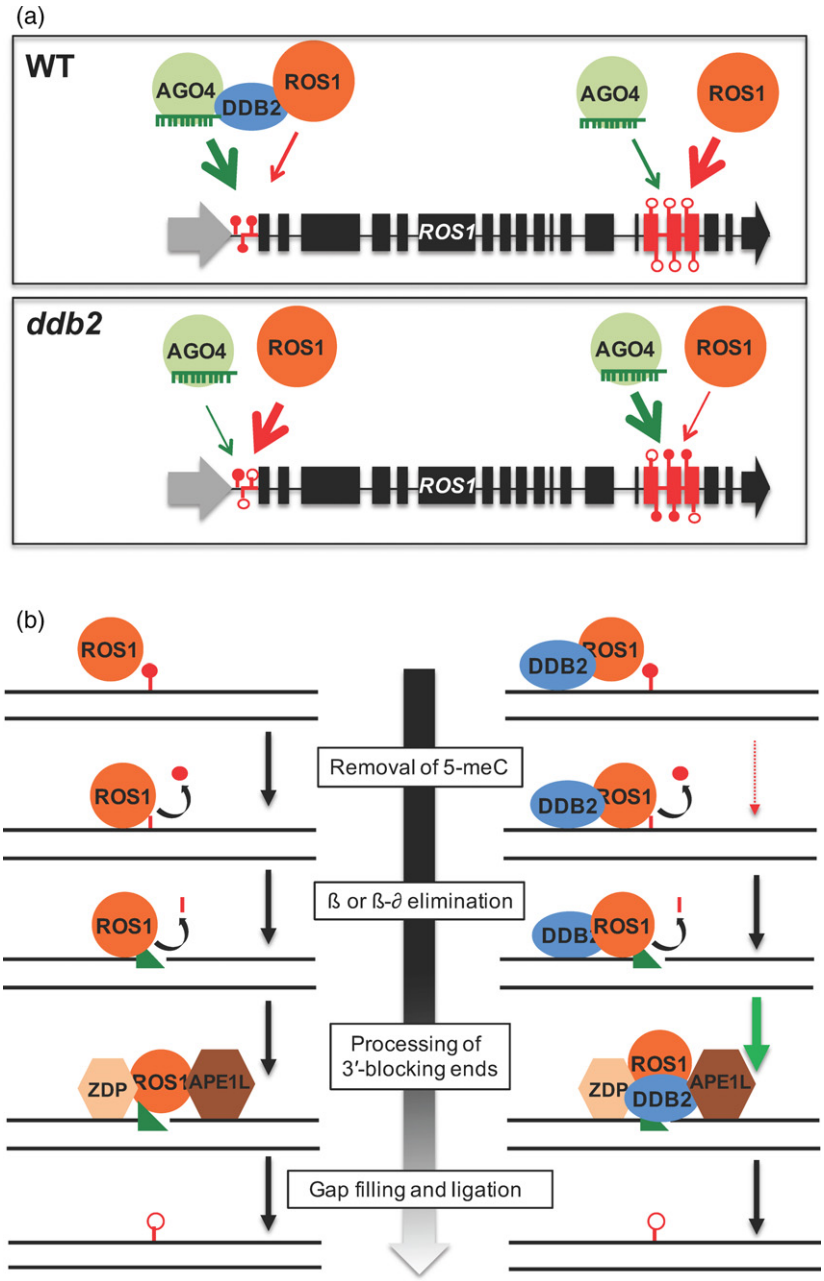

Figure 6. Model for DDB2 control of ROS1-mediated active DNA demethylation.
(a) DDB2, together with AGO4 and ROS1, act as regulators of *ROS1* expression. Schematic representation of the *ROS1* locus. The REP5 transposon is shown in grey. The P and D regulatory regions are highlighted in red. Top panel: at the P region in WT plants, DDB2 prevents active DNA demethylation by ROS1 (thin red arrow) allowing AGO4-mediated DNA methylation (thick green arrow). Conversely, ROS1 actively demethylates the D region. Bottom panel: in the absence of DDB2, active DNA demethylation and AGO4-mediated methylation are enhanced at the P and D loci, respectively, and *ROS1* expression increases.
(b) Control of active DNA demethylation. Left panel: current model. Right panel: proposed model in which DDB2 inhibits ROS1 5-meC DNA glycosylase activity (thin red arrow). Upon 5-meC excision, ROS1 cleaves the sugar phosphate backbone generating a single-nucleotide gap with either 3′-P or 3′-PUA ends (green triangle). DDB2 stimulates post-incision events through enhanced ZDP and APE1L activities (green arrow). Closed and open circles represent methylated and unmethylated cytosines, respectively.

ddb2 mutant plants may reflect a local increase in ROS1 activity. This hypomethylation correlates with the enhanced ROS1-binding identified in *ddb2* plants and with the loss of the DDB2 inhibitory effect of ROS1. Apparently, this *ddb2*-induced MEMS hypomethylation associated with *ROS1* overexpression challenges the model in which DNA methylation of the MEMS sequence restores *ROS1* expression to WT levels (Lei *et al.*, 2015; Williams *et al.*, 2015). However, it should be noted that DDB2 deficiency increases *ROS1* expression to well over WT levels (Figures 1b and S1c). Together, these observations suggest that the repressive effect of DDB2 on *ROS1* expression is not predominantly mediated by changes in MEMS DNA methylation. We propose that DDB2 has a dual function. First, through direct interaction with AGO4 and ROS1, stimulating methylation and inhibiting demethylation and second as a transcriptional repressor of *ROS1* expression. Interestingly, mammalian DDB2 has been reported as a transcriptional repressor of a constitutive gene (Minig *et al.*, 2009). Moreover, it is tempting to speculate that the association of DDB2 with ROS1 may influence its own stability since DDB2 is subjected to ubiquitin-mediated proteolytic degradation (Molinier *et al.*, 2008). An important question is why DDB2 is required to control the expression

© 2017 The Authors
The Plant Journal published by John Wiley & Sons Ltd and Society for Experimental Biology.,

of *ROS1*. One possibility is that DDB2 functions to fine-tune the MEMS methylstat in order to prevent genome-damaging effects. We propose a model (Figure 6a) in which DDB2 is recruited to the *ROS1* promoter region to avoid the accumulation of DNA demethylation intermediates arising from the cycling process of DNA methylation/demethylation at MEMS. Such recruitment, which might involve the capacity of DDB2 to detect altered conformations of DNA (Wittschieben *et al.*, 2005), stimulates the processing of such intermediates (Figure 6b), inhibits ROS1 demethylation activity, represses *ROS1* expression and stimulates RdDM-dependent DNA methylation. The net effect is a WT steady-state level of both DNA methylation and *ROS1* expression. In a *ddb2* mutant background, MEMS methylation decreases and *ROS1* expression increases over WT levels via the release of ROS1 activity. Interestingly, we found that a region located between exons 15 and 17 of the *ROS1* locus, called the D region, displays an enhanced DNA methylation level in *ddb2* mutant plants. This hypermethylation could be directly correlated with the enhanced level of *ROS1* expression and is possibly the result of transcription-coupled mechanisms involving MET1 (Teixeira and Colot, 2009; Miura *et al.*, 2009). Moreover, in *ddb2* mutant plants the methylation level of the D region is positively correlated with enhanced 24-nt siRNA abundance and AGO4 binding. We identified that this region is under the influence of both RdDM and ROS1. Thus, the decrease in MEMS DNA methylation might be counterbalanced by the RdDM-dependent hypermethylation of the D region leading to restoration and/or enhanced *ROS1* expression. Consistent with this, plants impaired in RdDM exhibit both MEMS and D region hypomethylation (Williams *et al.*, 2015). Loss of DNA methylation at the P region and hypermethylation at the D region were also observed in *met1* mutant plants, but unlike in the *ddb2* mutant plants *ROS1* expression was strongly reduced (Rigal *et al.*, 2012; Williams *et al.*, 2015). This discrepancy between both mutants could be explained by the minimal level of DNA methylation maintained at MEMS, probably due to the influence of DDB2 on *de novo* DNA methylation (Schalk *et al.*, 2016). This may reflect that RdDM takes over DNA demethylation at this particular region and that DDB2 acts as a dual regulator. In addition, our results allow us to propose that the D region may serve as back-up regulatory MEMS to maintain, restore or enhance *ROS1* expression, especially when DDB2 homeostasis varies.

Elevated *ROS1* expression was also detected in plants defective for the expression of the cognate GGR factors CEN2 and RAD10 (Schalk and Molinier, 2016). Contrary to the *ddb2* mutant plants, *cen2* plants exhibit hypermethylation of the MEMS in agreement with the already published model (Lei *et al.*, 2015; Williams *et al.*, 2015). CEN2 is part of the XPC complex that recognizes bulky DNA lesions during the NER pathway. CEN2 stabilizes XPC on chromatin and inhibits ubiquitin-dependent degradation of DDB2, enhancing its retention on chromatin (Matsumoto *et al.*, 2015). Therefore, the enrichment of DDB2 on chromatin in *cen2* mutant plants would entail that hypermethylation of the MEMS is be due to the inhibition of ROS1 chromatin loading/activity.

Given that *ROS1* expression is under the complex control of different factors such as the DNA methyltransferases MET1, CMT3, DRM2 and the H3K9 histone methyl transferase/demethylase KYP (kryptonite), IBM1 (increase in *BONSAI* methylation 1), respectively (Rigal *et al.*, 2012) it would be of great interest to establish how DDB2 interconnects with these factors. Additionally, it is likely that expression of ROS1 is not only regulated by DNA methylation. The fact that recovery of methylation at the P locus in *ddb2 nrpd1* double mutants does not restore *ROS1* expression to WT levels (Figure S1b) supports this idea. It should also be considered that certain growth conditions (i.e. upon UV exposure) that influence DDB2 homeostasis/dynamics may also affect *ROS1* expression. Indeed, it has been reported that upon UV exposure the steady-state level of DDB2 mRNA increases (Al Khateeb and Schroeder, 2009; Biedermann and Hellmann, 2010) while ROS1 decreases (Qüesta *et al.*, 2013). On the other hand *ros1* mutants show increased photorepair (Qüesta *et al.*, 2013), which suggests that such *ROS1* repression, mediated either by upregulation of DDB2 or by other factors, is important for a coordinated response to UV-induced DNA damage. This correlation emphasizes that contents of DDB2 and ROS1 are closely related and support the hypothesis that environmental stress may also control the DNA methylation landscape in a DDB2–ROS1-dependent manner.

DDB2 plays a key role in DNA methylation dynamics

Our study unveils DDB2 as an important factor controlling active DNA demethylation, adding a new level of knowledge about the complex regulation of DNA methylation dynamics. Actually, *ddb2* mutant plants exhibit genome-wide alterations in DNA methylation (Schalk *et al.*, 2016). These changes are explained by the misregulation of the local control of *de novo* DNA methylation by the DDB2–AGO4–siRNA complex and also by misregulation of *ROS1* and *DML3* expression (Schalk *et al.*, 2016). In the course of this study we showed that ROS1 forms, *in vivo*, a complex with AGO4 and DDB2. Therefore, DDB2-dependent control of the local abundance of 24-nt siRNA (Schalk *et al.*, 2016) and of the demethylation activities provides compelling evidence that DDB2 directly interconnects the RdDM and the active DNA demethylation pathways. More generally we could consider that DDB2 plays a regulatory role in the control of DNA methylation dynamics, ensuring efficient shaping of the methylome by interconnecting/coordinating different pathways.

© 2017 The Authors
The Plant Journal published by John Wiley & Sons Ltd and Society for Experimental Biology.,

EXPERIMENTAL PROCEDURES

Plant material

Arabidopsis thaliana plants used in this study are of the Columbia-0 ecotype (Col) for *ddb2-3*, *nrpd1*, *rdr2* (Schalk *et al.*, 2016), *ago4-1* (Zilberman *et al.*, 2003), *ros1* (SALK_045303) and *ddb2-3 DDB2-FLAG* (Schalk *et al.*, 2016) and in the Nossen ecotype (No) for *ddb2-2* (Molinier *et al.*, 2008).

Generation of transgenic plants

The genomic DNA (ATG to stop codon) of Arabidopsis *ROS1* was amplified by PCR using primers described in Schalk *et al.* (2016). *ROS1* genomic DNA was sequenced and cloned between the *Nco*I and *Avr*II sites into the pOEX2 vector (Molinier *et al.*, 2004). The *pOEX2 ROS1-FLAG* plasmid was mobilized into *Agrobacterium tumefaciens* to transform *ros1-3* and *ddb2-3* Arabidopsis plants. The *DDB2-FLAG* construct (Schalk *et al.*, 2016) was used to transform *rdr2* plants.

Immunoprecipitation assays

One gram of 10-day-old *ros1* ROS1-FLAG-expressing seedlings was used to extract total soluble proteins in 3 ml of IP buffer (Pazhouhandeh *et al.*, 2011). Anti-FLAG gel affinity (Sigma, http://www.sigmaaldrich.com/) was used for immunoprecipitation. The precipitate was washed four times in IP buffer, resuspended in 50 μl of SDS sample buffer and heated for 3 min at 100°C prior to immunoblotting. Anti-FLAG horseradish peroxidase (Sigma; 1:10 000 dilution) was used to detect the ROS1-FLAG protein.

Protein extraction and immunoblotting

Whole protein extracts were prepared as described in Molinier *et al.* (2008). Twenty micrograms of total protein was separated by 8% SDS gel and blotted as described in Molinier *et al.* (2008). Anti-AtDDB2 antibody (Molinier *et al.*, 2008; 1:2000 dilution), anti-AGO4 (Garcia *et al.*, 2012; 1:4000 dilution) and anti-ROS1Ct (Abiocode, https://www.abiocode.com/; 1:2000 dilution) were used.

McrBC treatment

Genomic DNA (1.5 μg) was digested with the McrBC enzyme (New England Biolabs, https://www.neb.com/) for 8 h at 37°C. Undigested genomic DNA (1.5 μg) was used as a control. DNA methylation levels at the P and D regions of *ROS1* were determined by real-time PCR and percentage DNA methylation was calculated as described in Schalk *et al.* (2016). Experiments were done in triplicate using independent biological samples. Three technical replicates were performed for each independent biological sample. Primers are listed in Table S2.

Chromatin immunoprecipitation

The ChIP experiments were performed according Pazhouhandeh *et al.* (2011) using 10-day-old seedlings grown *in vitro* (Roudier *et al.*, 2011). The immunoprecipitated DNA was analysed by real-time qPCR. Experiments were done in triplicate using independent biological samples. Three technical replicates were performed for each independent biological sample.

Quantitative PCR

Quantitative PCR was performed using a LightCycler 480 and LightCycler 480 SYBR green I Master mix (Roche, http://www.roche.com/) following the manufacturer's instructions. Normalization was performed relative to the housekeeping genes *Actin2*, *Ubiquino-cytochrome C Reductase* and *Hexokinase 1* as described in Schalk *et al.* (2016).

Enzyme assays

Double-stranded oligonucleotides (20 nM) were incubated at the specified temperature in a reaction mixture containing 50 mM 2-amino-2-(hydroxymethyl)-1,3-propanediol (TRIS)–HCl pH 8.0, 1 mM DTT, 0.1 mg ml^{-1} BSA and the corresponding amount of the indicated proteins in a total volume of 50 μl. Reactions mixtures containing APE1L or LIG1 also included 2 mM ATP and either 2 mM or 5 mM $MgCl_2$, respectively. Reactions were stopped by adding 20 mM EDTA, 0.6% sodium dodecyl sulfate and 0.5 mg ml^{-1} proteinase K, and the mixtures were incubated at 37°C for 30 min. DNA was extracted with phenol/chloroform/isoamyl alcohol (25:24:1) and ethanol precipitated at −20°C in the presence of 0.3 mM NaCl and 16 μg ml^{-1} glycogen. Samples were resuspended in 10 μl of 90% formamide, heated at 95°C for 5 min, and separated in a 12% denaturing polyacrylamide gel containing 7 M urea. Fluorescein or Alexa Fluor-labeled DNA was visualized using the fluorescence mode of an FLA-5100 imager and analyzed using Multigauge software (Fujifilm, http://www.fujifilm.com/).

ACKNOWLEDGEMENTS

This work was supported by the Spanish Ministry of Science and Innovation and the European Regional Development Fund under grant BFU2016-80728-P (to TRA) and by the Junta de Andalucía and the European Regional Development Fund under grant P11-CVI-7576 (to TRA). We thank members of our laboratories for helpful discussions and advice.

CONFLICT OF INTEREST

The authors have no conflict of interest to declare.

SUPPORTING INFORMATION

Additional Supporting Information may be found in the online version of this article.

Figure S1. DNA methylation profiles at the *ROS1* locus.

Figure S2. Inhibition of ROS1 activity by DDB2 is not due to DNA-binding competition.

Figure S3. DDB2 has no effect on the apurinic/apyrimidinic endonuclease activity of APE1L and the DNA ligase activity of LIG1.

Table S1. The DNA sequences of oligonucleotides used as substrates.

Table S2. List of primers used for quantitative PCR.

Data S1. Experimental procedures.

REFERENCES

Al Khateeb, W.M. and Schroeder, D.F. (2009) Overexpression of Arabidopsis damaged DNA binding protein 1A (DDB1A) enhances UV tolerance. *Plant Mol. Biol.* **4**, 371–383.

Biedermann, S. and Hellmann, H. (2010) The DDB1a interacting proteins ATCSA-1 and DDB2 are critical factors for UV-B tolerance and genomic integrity in *Arabidopsis thaliana*. *Plant J.* **3**, 404–415.

Chu, G. and Chang, E. (1988) Xeroderma pigmentosum group E cells lack a nuclear factor that binds to damaged DNA. *Science*, **4878**, 564–567.

Córdoba-Cañero, D., Roldán-Arjona, T. and Ariza, R.R. (2011) Arabidopsis ARP endonuclease functions in a branched base excision DNA repair pathway completed by LIG1. *Plant J.* **68**, 693–702.

© 2017 The Authors

Cuerda-Gil, D. and Slotkin, R.K. (2016) Non-canonical RNA-directed DNA methylation. *Nat. Plants*, **11**, 16163.

Duan, C.G., Wang, X., Tang, K. *et al.* (2015) MET18 connects the cytosolic iron-sulfur cluster assembly pathway to active DNA demethylation in Arabidopsis. *PLoS Genet.* **10**, e1005559.

Garcia, D., Garcia, S., Pontier, D., Marchais, A., Renou, J.P., Lagrange, T. and Voinnet, O. (2012) Ago hook and RNA helicase motifs underpin dual roles for SDE3 in antiviral defense and silencing of nonconserved intergenic regions. *Mol. Cell*, **48**, 109–120.

Kim, J.Y., Kwak, K.J., Jung, H.J., Lee, H.J. and Kang, H. (2010) MicroRNA402 affects seed germination of *Arabidopsis thaliana* under stress conditions via targeting DEMETER-LIKE Protein3 mRNA. *Plant Cell Physiol.* **6**, 1079–1083.

Law, J.A. and Jacobsen, S.E. (2010) Establishing, maintaining and modifying DNA methylation patterns in plants and animals. *Nat. Rev. Genet.* **11**, 204–220.

Lee, J., Jang, H., Shin, H., Choi, W.L., Mok, Y.G. and Huh, J.H. (2014) AP endonucleases process 5-methylcytosine excision intermediates during active DNA demethylation in Arabidopsis. *Nucleic Acids Res.* **18**, 11408–11418.

Lei, M., Zhang, H., Julian, R., Tang, K., Xie, S. and Zhu, J.K. (2015) Regulatory link between DNA methylation and active demethylation in Arabidopsis. *Proc. Natl Acad. Sci. USA* **11**, 3553–3557.

Li, Y., Córdoba-Cañero, D., Qian, W., Zhu, X., Tang, K., Zhang, H., Ariza, R.R., Roldán-Arjona, T. and Zhu, J.K. (2015a) An AP endonuclease functions in active DNA demethylation and gene imprinting in Arabidopsis. *PLoS Genet.* **11**, e1004905.

Li, Y., Duan, C.G., Zhu, X., Qian, W. and Zhu, J.K. (2015b) A DNA ligase required for active DNA demethylation and genomic imprinting in Arabidopsis. *Cell Res.* **25**, 757–760.

Martínez-Macías, M.I., Qian, W., Miki, D. *et al.* (2012) A DNA 3′ phosphatase functions in active DNA demethylation in Arabidopsis. *Mol. Cell*, **3**, 357–370.

Martínez-Macías, M.I., Córdoba-Cañero, D., Ariza, R.R. and Roldán-Arjona, T. (2013) The DNA repair protein XRCC1 functions in the plant DNA demethylation pathway by stimulating cytosine methylation (5-meC) excision, gap tailoring, and DNA ligation. *J. Biol. Chem.* **8**, 5496–55505.

Matsumoto, S., Fischer, E.S., Yasuda, T. *et al.* (2015) Functional regulation of the DNA damage-recognition factor DDB2 by ubiquitination and interaction with xeroderma pigmentosum group C protein. *Nucleic Acids Res.* **3**, 1700–1713.

Matzke, M.A. and Mosher, R.A. (2014) RNA-directed DNA methylation: an epigenetic pathway of increasing complexity. *Nat. Rev. Genet.* **15**, 394–408.

Mi, S., Cai, T., Hu, Y. *et al.* (2008) Sorting of small RNAs into Arabidopsis argonaute complexes is directed by the 5′ terminal nucleotide. *Cell*, **1**, 116–127.

Minig, V., Kattan, Z., van Beeumen, J., Brunner, E. and Becuwe, P. (2009) Identification of DDB2 protein as a transcriptional regulator of constitutive SOD2 gene expression in human breast cancer cells. *J. Biol. Chem.* **21**, 14165–14176.

Miura, A., Nakamura, M., Inagaki, S., Kobayashi, A., Saze, H. and Kakutani, T. (2009) An Arabidopsis jmjC domain protein protects transcribed genes from DNA methylation at CHG sites. *EMBO J.* **8**, 1078–1086.

Molinier, J., Ramos, C., Fritsch, O. and Hohn, B. (2004) CENTRIN2 modulates homologous recombination and nucleotide excision repair in Arabidopsis. *Plant Cell*, **6**, 1633–1643.

Molinier, J., Lechner, E., Dumbliauskas, E. and Genschik, P. (2008) Regulation and role of Arabidopsis CUL4-DDB1A-DDB2 in maintaining genome integrity upon UV stress. *PLoS Genet.* **4**, e1000093.

Morales-Ruiz, T., Ortega-Galisteo, A.P., Ponferrada-Marin, M.I., Martinez-Macias, M.I., Ariza, R.R. and Roldan-Arjona, T. (2006) *DEMETER* and *REPRESSOR OF SILENCING 1* encode 5-methylcytosine DNA glycosylases. *Proc. Natl Acad. Sci. USA* **103**, 6853–6858.

Parrilla-Doblas, J.T., Ponferrada-Marin, M.I., Roldan-Arjona, T. and Ariza, R.R. (2013) Early steps of active DNA demethylation initiated by ROS1 glycosylase require three putative helix-invading residues. *Nucleic Acids Res.* **41**, 8654–8664.

Pazhouhandeh, M., Molinier, J., Berr, A. and Genschik, P. (2011) MSI4/FVE interacts with CUL4-DDB1 and a PRC2-like complex to control epigenetic regulation of flowering time in Arabidopsis. *Proc. Natl Acad. Sci. USA* **108**, 3430–3435.

Pecinka, A. and Mittelsten Scheid, O. (2012) Stress-induced chromatin changes: a critical view on their heritability. *Plant Cell Physiol.* **5**, 801–808.

Penterman, J., Uzawa, R. and Fischer, R.L. (2007) Genetic interactions between DNA demethylation and methylation in Arabidopsis. *Plant Physiol.* **4**, 1549–1557.

Ponferrada-Marín, M.I., Roldán-Arjona, T. and Ariza, R.R. (2009) ROS1 5-methylcytosine DNA glycosylase is a slow-turnover catalyst that initiates DNA demethylation in a distributive fashion. *Nucleic Acids Res.* **37**, 4264–4274.

Qüesta, J.I., Fina, J.P. and Casati, P. (2013) DDM1 and ROS1 have a role in UV-B induced- and oxidative DNA damage in *A. thaliana*. *Front. Plant Sci.* **4**, 420.

Rigal, M., Kevei, Z., Pélissier, T. and Mathieu, O. (2012) DNA methylation in an intron of the IBM1 histone demethylase gene stabilizes chromatin modification patterns. *EMBO J.* **13**, 2981–2993.

Roudier, F., Ahmed, I., Bérard, C. *et al.* (2011) Integrative epigenomic mapping defines four main chromatin states in Arabidopsis. *EMBO J.* **30**, 1928–1938.

Schalk, C. and Molinier, J. (2016) Global Genome Repair factors controls DNA methylation patterns in Arabidopsis. *Plant Signal. Behav.* **12**, e1253648.

Schalk, C., Drevensek, S., Kramdi, A. *et al.* (2016) DNA DAMAGE BINDING PROTEIN 2 (DDB2) shapes the DNA methylation landscape. *Plant Cell* **pii**, tpc.00474.2016.

Schalk, C., Cognat, V., Graindorge, S., Vincent, T., Voinnet, O. and Molinier, J. (2017) Small RNA-mediated repair of UV-induced DNA lesions by the DNA DAMAGE BINDING protein 2 and ARGONAUTE 1. *Proc. Natl Acad. Sci. USA* **14**, E2965–E2974.

Tang, K., Lang, Z., Zhang, H. and Zhu, J.K. (2016) The DNA demethylase ROS1 targets genomic regions with distinct chromatin modifications. *Nat. Plants*, **11**, 16169.

Teixeira, F.K. and Colot, V. (2009) Gene body DNA methylation in plants: a means to an end or an end to a means? *EMBO J.* **8**, 997–998.

Virdi, K.S., Laurie, J.D., Xu, Y.Z. *et al.* (2015) Arabidopsis MSH1 mutation alters the epigenome and produces heritable changes in plant growth. *Nat. Commun.* **6**, 6386.

Wang, X., Li, Q., Yuan, W., Cao, Z., Qi, B., Kumar, S., Li, Y. and Qian, W. (2016) The cytosolic Fe-S cluster assembly component MET18 is required for the full enzymatic activity of ROS1 in active DNA demethylation. *Sci. Rep.* **6**, 26443.

Williams, B.P., Pignatta, D., Henikoff, S. and Gehring, M. (2015) Methylation-sensitive expression of a DNA demethylase gene serves as an epigenetic rheostat. *PLoS Genet.* **3**, e1005142.

Wittschieben, B.Ø., Iwai, S. and Wood, R.D. (2005) DDB1-DDB2 (xeroderma pigmentosum group E) protein complex recognizes a cyclobutane pyrimidine dimer, mismatches, apurinic/apyrimidinic sites, and compound lesions in DNA. *J. Biol. Chem.* **280**, 39982–39989.

Zemach, A., Kim, M.Y., Hsieh, P.H., Coleman-Derr, D., Eshed-Williams, L., Thao, K., Harmer, S.L. and Zilberman, D. (2013) The Arabidopsis nucleosome remodeler DDM1 allows DNA methyltransferases to access H1-containing heterochromatin. *Cell*, **1**, 193–205.

Zhu, J.K. (2009) Active DNA demethylation mediated by DNA glycosylases. *Annu. Rev. Genet.* **43**, 143–166.

Zilberman, D., Cao, X. and Jacobsen, S.E. (2003) ARGONAUTE4 control of locus-specific siRNA accumulation and DNA and histone methylation. *Science*, **299**, 716–719.

© 2017 The Authors
The Plant Journal published by John Wiley & Sons Ltd and Society for Experimental Biology.,